



Contents lists available at **SCCE**

Journal of Soft Computing in Civil Engineering

Journal homepage: [www.jsoftcivil.com](http://www.jsoftcivil.com)



## A Grey-Fuzzy Based Approach for the Optimization of Corrosion Resistance of Rebars Coated with Ternary Electroless Nickel Coatings

Arkadeb Mukhopadhyay<sup>1</sup>, Sarmila Sahoo<sup>2\*</sup>

1. Assistant Professor, Department of Mechanical Engineering, Birla Institute of Technology, Mesra, Ranchi – 835215, India

2. Associate Professor, Department of Civil Engineering, Heritage Institute of Technology, Kolkata – 700107, India

Corresponding author: [sarmila.sahoo@heritageit.edu](mailto:sarmila.sahoo@heritageit.edu)

<https://doi.org/10.22115/SCCE.2022.326903.1401>

### ARTICLE INFO

Article history:

Received: 28 January 2022

Revised: 29 April 2022

Accepted: 02 June 2022

Keywords:

Ni-W-P;

Ni-Cu-P;

Electroless;

Rebar;

Grey-fuzzy optimization;

Corrosion.

### ABSTRACT

Corrosion is an important phenomenon that occurs at concrete-rebar interface and affects the life of structures in coastal environments. Fe-600 grade steel is used in India for construction purposes especially in seismic zones. Hence, the corrosion of the rebars and its optimization is necessary to increase the lifetime of structures. In this regard, the present investigation examines the applicability of electroless Ni-P based ternary coatings as candidates for corrosion protection and obtains an optimal bath formulation. Investigation of electrochemical corrosion phenomenon (potentiodynamic polarization) was carried out in 3.5% NaCl to simulate saline coastal environment. Ni-P coatings with Cu and W inclusion were considered due to their proven corrosion resistance. The bath constituents such as nickel sulphate (Ni source), sodium hypophosphite (reducing agent and source of P) and the tungsten / copper concentration were varied to get various elemental composition following a sequential experimental design i.e. Taguchi's L<sub>9</sub> orthogonal array. A grey based fuzzy reasoning approach was proposed to optimize the bath and achieve enhanced corrosion resistance. The optimized coatings exhibited initiation of passivation which could prove to be beneficial for the health of the structure in the long-run. A noble corrosion potential and lower corrosion current density could be obtained in the coated rebars from the grey fuzzy methodology.

How to cite this article: Mukhopadhyay A, Sahoo S. A grey-fuzzy based approach for the optimization of corrosion resistance of rebars coated with ternary electroless nickel coatings. *J Soft Comput Civ Eng* 2022;6(2):107–127. <https://doi.org/10.22115/scce.2022.326903.1401>

2588-2872/ © 2022 The Authors. Published by Pouyan Press.

This is an open access article under the CC BY license (<http://creativecommons.org/licenses/by/4.0/>).



## 1. Introduction

A significant attention is required for corrosion prevention of rebars used in construction, and structures used in coastal areas [1–3]. Due to the porosity of concrete, the penetration of corrosive media is inevitable causing degradation in the lifetime of structures and a consequent increase in maintenance expenditure [4–6]. Pitting attack of chlorides is encountered by rebars in marine environment due to attack of harsh chloride species [7–9]. Although there is a passivating layer formation on rebars in alkaline environment, this layer gets damaged beyond critical threshold limit of chloride ions [10–12]. The degradation is further aided by carbonation [13,14].

There are several ways to counteract the corrosion of rebars. Self-healing capabilities may be induced in concrete containing admixtures [15–20]. A suitable grade of steel may be also selected to enhance corrosion performance. Austenitic grade steel has high corrosion resistance in seawater conditions [21]. A compact and dense passivating layer form on chromium modified steel [22].

Surface engineering plays a key role in corrosion protection of rebars in aggressive mediums [23]. A widely investigated coating variant are enamel and epoxy-based coatings [24–26] because they have the capability of providing protection over significant time duration. Pure enamel-based coatings were seen to provide corrosion protection in chloride environment over a very long period of 244 days [27]. It was also recommended that enamel coatings should be handled carefully during transportation due to its tendency to get damaged. Another coating variant which has shown promising results are epoxy-based coatings. The epoxy coatings provide good bonding with mortar mixture and have high corrosion resistance [28]. Epoxy coatings show low permeability and hence do not allow infiltration of chloride species. Thus the coatings showed high corrosion resistance over a period of two years [29]. Nano-filler addition also improved the corrosion protection capability of the epoxy coatings [30,31]. Epoxy, enamel and duplex coating with inner layer as enamel and outer layer as epoxy coatings were investigated [32]. The duplex coating provided an improvement of 180% in corrosion resistance. Though in another study it was seen that epoxy coatings were not very effective in preventing expansion of corrosion and induces cracking if percent of defect area to rebar area exceeds 5% [26]. On the other hand, polypropylene fiber addition to concrete reduced crack width in epoxy coated rebars but there was no beneficial effect in metal loss arising out of corrosion [26]. Passivation and long-term corrosion resistance in chloride environment was also observed in galvanized rebars [33,34].

Electroless Ni-P coatings have high corrosion resistance and enhanced mechanical properties by virtue of its composition and microstructure [35–40]. Due to their proven corrosion resistance, Ni-P based binary and the ternary coatings have found wide industrial usage such as chemical carrying transports, oil and petrochemical industries, textiles and food processing [40]. Furthermore, the high P coatings are essentially low cost alternatives to nickel, stainless steel or monel alloys as construction material [40]. Electroless Ni-P coatings in simulated seawater condition have shown promising results [41]. Furthermore, Ni-P and some ternary variants were investigated in 3.5% NaCl using electrochemical tests [42]. The uncoated Fe-600 rebars showed

severe cracking due to chloride attack. On the other hand, Ni-W-P electroless coated rebars showed noble corrosion potential and low corrosion current density. Similar results were observed in 0.5 M H<sub>2</sub>SO<sub>4</sub> [43]. Bath optimization of electroless Ni-W-P and Ni-Cu-P coatings to achieve enhanced corrosion resistance of coated rebars in simulated seawater condition was also attempted to improve cost-effectivity of the process [44,45].

Careful observation reveals the fact that a significant attention is being given to enhance lifetime of rebars. The application of a protective coating layer can significantly improve corrosion resistance. Various coating methods have been used such as enamel, epoxy, duplex, electroless Ni-P, etc., to improve corrosion performance of rebars in chloride environment, sulphate attacks, carbonated solutions, etc. Recent studies have also reported soy-protein and corn-derived polyol coatings, as well as graphene modified epoxy coatings for corrosion protection of rebars [46,47]. Amongst all the coating variants, the electroless nickel coatings have been scarcely explored though they have tremendous potential, proven corrosion resistance and cost effective. Even though the Ni-P coatings have high corrosion resistance, their applicability to in the construction sector yet remains un-investigated. Furthermore, the electroless coatings follow the substrate roughness closely and thus would prove to be beneficial in coating ribbed rebars. The ribs provide good bonding at the interface of concrete and the reinforcement. In such a case, it is essential that the coating applied should follow the surface topography. The present work thus focuses on the enhancement of corrosion mitigation at concrete-rebar interface by the application of Ni-P based ternary coatings developed via the electroless route.

Electroless Ni-W-P and Ni-Cu-P coatings were deposited on Fe-600 grade rebars. The cost effectivity of the process is improved by focusing on the standardization of bath parameters to achieve enhanced corrosion resistance. Electrochemical method like potentiodynamic polarization (PDP) is used to find out corrosion current density ( $I_{\text{corr}}$ ) and corrosion potential ( $E_{\text{corr}}$ ). Bath parameter optimization is carried out in a quest to improve the cost-effectivity of the process. For this, an integrated grey-fuzzy approach is adopted and the results are compared with the existing literature. Coating characterization is carried out by observing the surface morphology under scanning electron microscope and the structure is determined using X-ray diffraction technique. Finally, the corroded specimens are also studied to investigate the corrosion mechanism.

## **2. Grey fuzzy optimization methodology**

Grey relational analysis (GRA) has been utilized in optimization of industrial processes as well as coating properties has been addressed in several studies [48–52]. It has proven capabilities of solving multi-response optimization problems and is recommended for its simplicity. Any information which is complete is termed white in the grey system. When there is no information, then it is termed as black. But the complex interrelationships between process parameters and responses in complex industrial problems are difficult to predict due to its vagueness. Such systems are termed as grey and are effectively dealt with using GRA. Fuzzy logics were introduced by Zadeh [53] and have the capability of predicting complex inter-relationships with vagueness and imprecise information. Therefore, the fuzzy logics coupled with GRA may prove

to be more efficient in process optimization. It could overcome the uncertainties introduced into the multi-performance index (MPI) due to the vagueness introduced by quality characteristics. Moreover, the Taguchi's S/N ratio method is an offline quality control technique and may be applied to the single response optimization problems [54–57]. But the present problem considers more than one response. Therefore, grey fuzzy reasoning approach may be more suitable to address the problem and yield a system with better performance characteristics due to its associated advantages [58–61]. Fuzzy logics coupled with analytic hierarchy process could be successfully utilized to assess the damage in reinforced concrete bridges [62]. The vagueness and uncertainty associated with simplified corrosion index could be well handled by fuzzy logics [62]. Thus, the present work also adopts fuzzy logics coupled with GRA to take into the uncertainties associated with GRA. The optimization process may be summarized as follows:

### 2.1. Normalization

The responses are initially normalized between 0 and 1. Due to the variation in ranges of values and units of responses, this step is carried out. Firstly, the  $E_{\text{corr}}$  is normalized as per higher-the-better criteria since the aim is to achieve a nobler value. The formula is given as follows [44,45]:

$$x_i^*(k) = \frac{x_i(k) - \min x_i(k)}{\max x_i(k) - \min x_i(k)} \quad (1)$$

The  $I_{\text{corr}}$  is normalized as per lower-the-better characteristics since the corrosion current density should have a lower value. The formula to calculate the same is [44,45]:

$$x_i^*(k) = \frac{\max x_i(k) - x_i(k)}{\max x_i(k) - \min x_i(k)} \quad (2)$$

In both Equation 1 and 2,  $x_i(k)$  represents the experimental value of corrosion parameters obtained at a combination of coating bath parameters. The terms  $\max x_i(k)$  and  $\min x_i(k)$  represent the maximum and minimum values amongst all the trial runs.

### 2.2. Finding grey relational coefficients

The grey relational coefficient (GRC) of each response resembles how near it is towards its optimal condition i.e. 1. The grey relational coefficient is calculated as [44,45]:

$$\xi_i(k) = \frac{\Delta_{\min} + r\Delta_{\max}}{\Delta_{0i}(k) + r\Delta_{\max}} \quad (3)$$

The term  $\Delta_{0i} = \|x_{0i}(k) - x_i^*(k)\|$  whereas  $\Delta_{\min}$  and  $\Delta_{\max}$  are the minimum value and maximum value respectively. The two grey relational coefficients correspond to  $E_{\text{corr}}$  and  $I_{\text{corr}}$  i.e.  $\xi_1$  and  $\xi_2$  respectively. The value of distinguishing coefficient (r) for the calculation is taken as 0.5 [44,45]. When the value of r is taken as 0.5, it has moderate distinguishing ability and hence 0.5 is adopted in most research works.

### 2.3. Fuzzification of the grey relational coefficients and finding grey fuzzy grade

Fuzzy logics are well suited for handling uncertainty in problems. The uncertainty in grey relational grade may be handled using grey fuzzy logic to find out MPI. The fuzzy logic system

comprises of membership functions. Such membership functions may be triangular, Gaussian, trapezoidal or sigmoidal. These membership functions are used by a fuzzifier to assign the GRCs a value between 0 and 1 i.e. the GRCs are then fuzzified. A set of pre-defined rules in the form of ‘IF premise, THEN conclusion’ are defined and they are invoked by fuzzy inference engine. This fuzzy inference system can be the Mamdani max-min type or a Takagi-Sugeno type. In the present work Mamdani system is adopted because of its simplicity. As the fuzzy inference engine is invoked, the grey fuzzy grade (GFG) in fuzzy form is obtained. Ultimately the defuzzifier converts the GFG into a crisp value. Defuzzification can be done by centroid method, max-membership method or weighted average method. Amongst these the centroid method is the most popular and has been used in the present work. The centroid method gives the crisp out as follows:

$$y_0 = \frac{\sum y \mu_{C_0}(y)}{\sum \mu_{C_0}(y)} \quad (4)$$

Where  $y_0$  is the crisp grade,  $\mu_{C_0}(y)$  is the membership function and  $y$  is the fuzzy value of grade.

#### 2.4. Carrying out confirmation tests and statistical analysis

After optimization, confirmation experiment is carried out. Here, a comparison is made between the GFG at optimal condition, an arbitrary run and an equation predicted GFG. The equation to predict GFG ( $\hat{\gamma}$ ) is [44,45]:

$$\hat{\gamma} = \gamma_m + \sum_{i=1}^{i=o} (\bar{\gamma}_i - \gamma_m) \quad (5)$$

The mean of all values of GFG is  $\gamma_m$ . At each optimal level of process parameters, the mean GFG is denoted as  $\bar{\gamma}_i$  and total design variables are denoted by  $o$  which in this study is 3. The closer the predicted GFG and experimentally obtained GFG, higher is the reliability of the optimization method. Furthermore, the confirmation test must also indicate an improvement in grade compared to any initial random test run which in most studies are taken to be the mid-value combination of process parameters. The final step of the optimization methodology is the statistical analysis to find out the impact or significance of the process parameters. In complex engineering problems or experimental designs, this is carried out using analysis of variance (ANOVA). The individual effect of each of the coating bath parameters can be determined using ANOVA. This significance can be identified either from the percentage contribution of a factor or analysing the F-ratio. At any confidence level  $\alpha$ , a higher F-ratio compared to that of tabulated values indicates significance of a parameter. The F-ratio is denoted as regression mean square to mean squared error ratio. The schematic of the entire optimization methodology is shown in Fig. 1. Compared to the GRA, the grey fuzzy analysis is more complex and takes more computational time. The grey fuzzy analysis requires a knowledge base and experience to form the rule base. Depending on the accuracy of rule base, the accuracy of the predicted results is affected. Though uncertainties are well handled by the fuzzy logics and therefore have been combined with GRA to ensure accuracy of the optimized results.

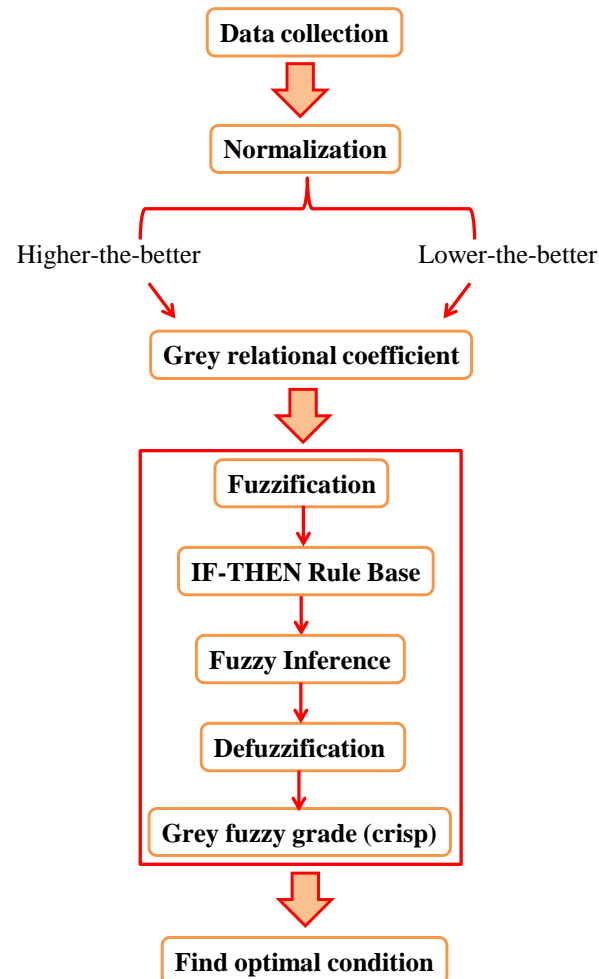


Fig. 1. Schematic of grey fuzzy analysis.

### 3. Materials and methods

Ni-Cu-P and Ni-W-P coatings were developed on Fe-600 grade rebars via the electroless route. In general electroless Ni coatings are either obtained by using sodium hypophosphite or sodium borohydride. The use of sodium hypophosphite as reducing agent leads to formation of Ni-P coating. A third element can be co-deposited along with Ni-P to achieve enhanced mechanical properties and corrosion resistance of Ni-P coatings. In this regard, Ni-Cu-P and Ni-W-P coatings have shown excellent corrosion resistance. Thus, the aforesaid coatings have been deposited onto Fe-600 grade rebars and the bath parameters have been optimized to achieve enhanced corrosion resistance. The rebars (20 mm nominal diameter and 2 mm thick) were ground to achieve centre line average roughness ( $R_a$ ) = 0.4  $\mu\text{m}$ . Thorough rinsing of the substrates were carried out in deionized water and degreased in acetone. This is done to remove surface impurities and oxide scales. Finally activation was carried out in HCl for a few seconds. Then the rebars were dipped in coating bath. The composition of coating bath for Ni-Cu-P and Ni-W-P coating is shown in Table 1. The coatings were in their as-deposited state and no further heat treatment was carried out. No mechanical agitation of the bath was carried out since alloy

coatings are deposited rather than composite variants. To achieve optimized coatings the chemicals were varied as shown in Table 2. Nine different combinations were used each for Ni-Cu-P and Ni-W-P following Taguchi’s L<sub>9</sub> orthogonal array.

The electrochemical corrosion tests were carried out to find out corrosion resistance of coated and uncoated rebars (GILL AC, ACM INSTRUMENTS). For this PDP was carried with E<sub>corr</sub> and I<sub>corr</sub> as the responses of optimization. A three electrode cell comprised of the working electrode as coated specimen, reference electrode as saturated calomel andauxillary electrode as platinum was used. To obtain simulated chlorinated environment, 3.5% NaCl was used. Stabilization of open circuit potential (OCP) was allowed for 15 minutes before the start of electrochemical tests. Polarization of working electrodes in cathodic and anodic direction took place at 1 mV/s (± 250 mV vs. OCP) and the time of tests was set automatically according to the polarization voltage by the software (ACM Analysis). The responses i.e. E<sub>corr</sub> and I<sub>corr</sub> were obtained by Tafel extrapolation using the same software.

The composition of coated rebars was studied by using energy dispersive X-ray spectroscopy (EDS). Analysis of surface characteristics was done by a scanning electron microscope (SEM) and the surface features were observed (JEOL, JSM 6390). Some characterizations were also done by a field emission scanning electron microscope (FESEM) and surface changes were observed (SIGMA – 300, ZEISS). Structure of coating was determined using X-ray diffraction (XRD) and it was carried out for 2θ values 20-80° (RIGAKU, SMART LAB). The XRD was carried out at 1°/min scan rate. Corrosion mechanism was studied by visualizing specimens under SEM and FESEM.

**Table 1**  
Composition of coating bath.

<b>Bath Composition</b>		
<b>Chemicals</b>	<b>Ni-W-P</b>	<b>Ni-Cu-P</b>
<b>Nickel Sulphate</b>	20-30	25-35
<b>Sodium Hypophosphite</b>	14-20	10-20
<b>Sodium Citrate</b>	35	15
<b>Ammonium Sulphate</b>	30	×
<b>Lactic Acid</b>	5	×
<b>Sodium Tungstate</b>	15-25	×
<b>Copper Sulphate</b>	×	0.3-0.7
<b>Deposition Conditions</b>		
<b>pH</b>	7-8	9.5
<b>Bath Volume</b>	200 ml	200 ml
<b>Deposition Temperature</b>	90 ± 2	85 ± 2
<b>Deposition Duration</b>	3 hours	3 hours
<b>Heat Treatment</b>	×	×
<b>Agitation</b>	×	×

**Table 2**

Levels of variation of design variables i.e. coating bath parameters.

Ni-W-P Coating					
Factors	Units	Code	Levels		
			1	2	3
Nickel sulphate	g/L	A	20*	25	30
Sodium hypophosphite	g/L	B	14	17	20*
Sodium tungstate	g/L	C	15	20	25*
*Initial test run combination ( $A_1B_3C_3$ )					
Ni-Cu-P Coating					
Factors	Units	Code	Levels		
			1	2	3
Nickel sulphate	g/L	A	25	30*	35
Sodium hypophosphite	g/L	B	10	15*	20
Copper Sulphate	g/L	C	0.3	0.5*	0.7
*Initial test run combination ( $A_2B_2C_2$ )					

## 4. Results and discussions

### 4.1. Optimization using grey fuzzy analysis

The results of corrosion tests are shown in Table 3. The data present in Table 3 is processed further. Initially normalization of  $E_{\text{corr}}$  is carried out using higher-the-better criteria (Eqn. 1) while  $I_{\text{corr}}$  is normalized using lower-the-better criteria (Eqn. 2). The normalized values are given in Table 4. The calculation for GRCs is carried out next as per Eqn. 3. To take care of the uncertainties introduced in the parameters due to usage of quality characteristics such as higher-the-better or lower-the-better, instead of finding grey relational grade (shown in Table 5), the GRCs are fuzzified. Triangular membership function is used for the same. For the GFG also, triangular membership function is chosen for its simplicity. The membership functions are shown in Fig. 2. Mamdani's max-min operation is performed by the fuzzy inference engine [58–63]. Finally, centre-of-gravity defuzzification method [58–63] is used to obtain the GFG (Eqn. 4) and shown in Table 6. The GFG in Table 6 has been assigned order between 1 to 9. Highest GFG has been assigned order since it is nearer to optimized value whereas the lowest GFG has been assigned order 9. The GFG is an indicator of the MPI and further optimization is carried out using the tabulated values. The 25 IF-ELSE rules used to invoke the fuzzy inference engine take the form:

Rule1: IF  $\xi_1$  is Very small AND  $\xi_2$  is Very small THEN Grade is Smallest

Rule 2: IF  $\xi_1$  is Small AND  $\xi_2$  is Small THEN Grade is Small

.

.

Rule 25: IF  $\xi_1$  is Very high AND  $\xi_2$  is Very high THEN Grade is Highest

After processing of data, the main effects plot is found out and shown in Fig. 3 and Fig. 4 for Ni-W-P and Ni-Cu-P coating respectively for the GFG given in Table 6. The optimal bath parameter combination predicted by grey fuzzy analysis is  $A_3B_2C_2$  for Ni-W-P and  $A_1B_1C_1$  for Ni-Cu-P coated rebar. The mean response table for GFG is tabulated in Table 7. The mean response of GFG is obtained by finding the average of GFG at a particular level for each of the process parameters. The response table (Table 7) has delta values which is the difference between highest and lowest value of mean GFG in a column. Based on this difference, ranks are assigned. The factor showing the highest difference is assigned rank 1 while the lowest has been assigned rank 3. Table 7 indicates sodium tungstate (Rank 1) to be most influential parameter followed by sodium hypophosphite (Rank 2) and nickel sulphate (Rank 3). On the other hand, for Ni-Cu-P coated rebar, nickel sulphate is more influential (Rank 1) followed by copper sulphate (Rank 2) and sodium hypophosphite (Rank 3). Similar results were obtained by Roy and Sahoo [64] for corrosion performance optimization of Ni-W-P which considered heat treatment temperature also along with the coating bath parameters considered in the present work.

**Table 3**  
Results of corrosion tests.

Sl. No.	Ni-W-P		Ni-Cu-P	
	$E_{corr}$ (mV vs. SCE)	$I_{corr}$ ( $\mu A/cm^2$ )	$E_{corr}$ (mV vs. SCE)	$I_{corr}$ ( $\mu A/cm^2$ )
1	-449	5.9	-350	0.4
2	-255	0.1	-301	3.05
3	-391	0.5	-416	3.6
4	-465	0.3	-435	4.9
5	-271	0.05	-455	13.5
6	-404	3.28	-433	0.7
7	-297	1.8	-436	14
8	-362	0.71	-558	4.7
9	-360	0.07	-466	17.9

#### 4.2. Confirmation test

Confirmatory experiment is done to compare the optimal values with initial test parameters which are shown in Table 8. The confirmation test also predicts a grade using Eqn 5. This predicted grade should be in close correlation with the experimentally obtained GFG to validate successful utilization of the optimization algorithm. When compared with the GFG of initial test run, at the optimized condition, there has been an increase in 5.9% and 44.03% of GFG for Ni-Cu-P and Ni-W-P coated rebars respectively. Thus, optimization leads to improvement in corrosion performance of electroless coated rebars. Further, the GFG is also predicted at optimal condition using Eqn. 5. The predicted GFG for both Ni-Cu-P and Ni-W-P coated rebar are in accordance with the experimental results. The comparison of optimized results is compared with bare rebars and the results are shown in Table 9. It may be seen that a significant improvement in corrosion resistance takes place on application of Ni-Cu-P or Ni-W-P coatings. The coated rebars

have nobler  $E_{corr}$  and lower  $I_{corr}$  compared to bare rebars. Maximum mitigation of rebar corrosion is achieved by application of Ni-W-P coating and hence recommended.

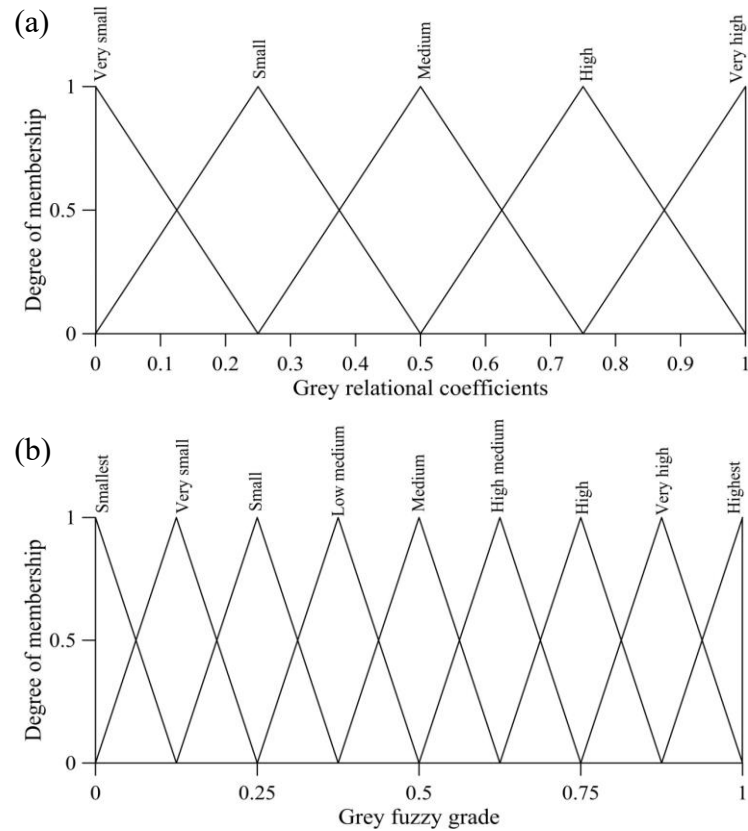


Fig. 2. Membership function of (a) grey relational coefficients and (b) grey fuzzy grade [63].

**Table 4**  
Normalized results of corrosion tests.

Sl. No.	Ni-W-P		Ni-Cu-P	
	Normalized $E_{corr}$	Normalized $I_{corr}$	Normalized $E_{corr}$	Normalized $I_{corr}$
1	0.0762	0.0000	0.8093	1.0000
2	1.0000	0.9915	1.0000	0.8486
3	0.3524	0.9231	0.5525	0.8171
4	0.0000	0.9573	0.4786	0.7429
5	0.9238	1.0000	0.4008	0.2514
6	0.2905	0.4479	0.4864	0.9829
7	0.8000	0.7009	0.4747	0.2229
8	0.0000	0.8872	0.0000	0.7543
9	0.5000	0.9966	0.3580	0.0000

**Table 5**

Grey relational coefficients of corrosion tests.

Sl. No.	Ni-W-P		Ni-Cu-P	
	GRC $E_{corr}$	GRC $I_{corr}$	GRC $E_{corr}$	GRC $I_{corr}$
1	0.351	0.333	0.724	1.000
2	1.000	0.983	1.000	0.768
3	0.436	0.867	0.528	0.732
4	0.333	0.921	0.490	0.660
5	0.868	1.000	0.455	0.400
6	0.413	0.475	0.493	0.967
7	0.714	0.626	0.488	0.391
8	0.333	0.816	0.333	0.670
9	0.500	0.993	0.438	0.333

**Table 6**

Grey fuzzy grade of corrosion tests.

Sl. No.	Ni-W-P		Ni-Cu-P	
	GFG	Order	GFG	Order
1	0.353	9	0.858	2.000
2	0.953	1	0.876	1.000
3	0.645	5	0.631	4.000
4	0.627	6	0.569	5.000
5	0.891	2	0.416	8.000
6	0.433	8	0.722	3.000
7	0.663	4	0.434	7.000
8	0.590	7	0.501	6.000
9	0.745	3	0.384	9.000

**Table 7**

Response table for means of the MPI i.e. GFG.

Ni-W-P coated rebars			
Level	A	B	C
1	0.6503	0.5477	0.4587
2	0.6503	0.8113	0.775
3	0.666	0.6077	0.733
Delta	0.0157	0.2637	0.3163
Rank	3	2	1
Average GFG = 0.656			
Ni-Cu-P coated rebars			
Level	A	B	C
1	0.7883	0.6203	0.6937
2	0.569	0.5977	0.6097
3	0.4397	0.579	0.4937
Delta	0.3487	0.0413	0.2
Rank	1	3	2
Average GFG = 0.599			

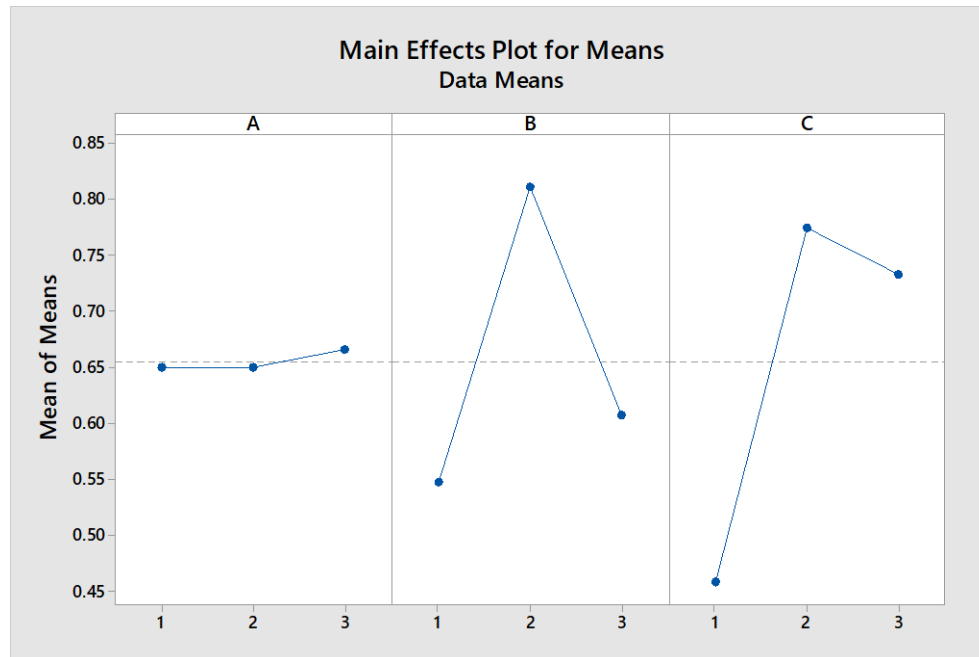


**Fig. 3.** Main effects plot of GFG of Ni-W-P coating.

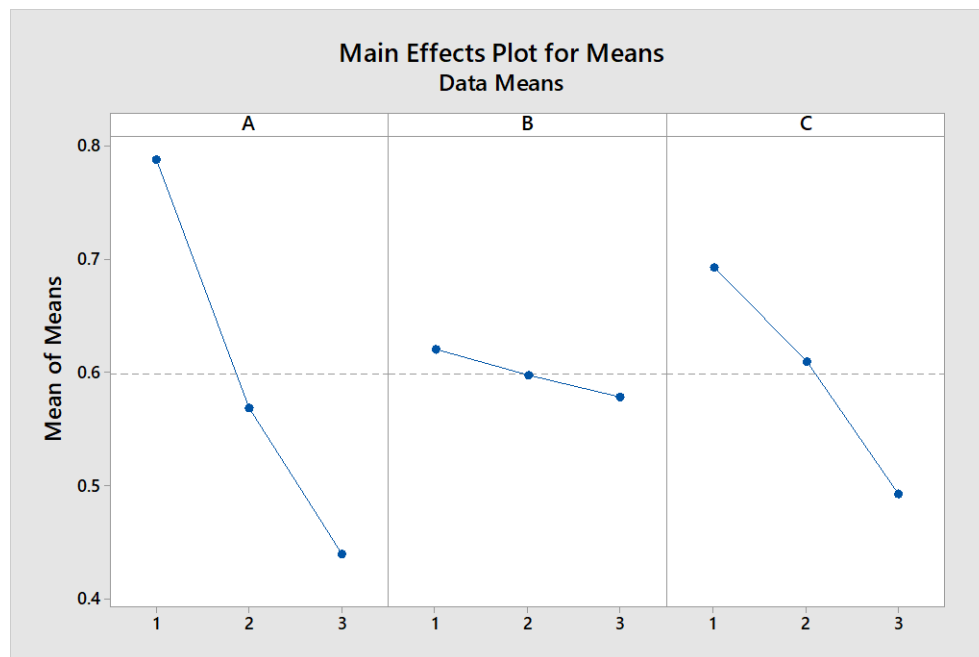


**Fig. 4.** Main effects plot of GFG of Ni-Cu-P coating.

### 4.3. Analysis of variance

The statistical significance of coating bath parameters on the PDP parameters is determined using ANOVA and shown in Table 10. In Table 10, DF, Adj SS and Adj MS denotes degree of freedom of experiment, adjusted sum of squares and adjusted mean square respectively. The F-ratio in Table 10 is the ratio of mean square of regression and the mean squared error. A higher ratio denotes higher contribution of a factor. The term 'Total' denotes the sum of adjusted sum of squares and percent contribution in a column while the term 'Error' denotes variability within

groups and accounts for the lack of goodness of fit. A very high contribution of 59.37% is revealed for sodium tungstate in influencing the MPI for Ni-W-P coated rebars. In Ni-W-P coatings, the presence of W has a corrosion mitigating effect [64]. Whereas 67.20% contribution is seen for nickel sulphate in case of Ni-Cu-P coated rebars. The concentration of nickel sulphate controls the nickel content in the coatings. Roy and Sahoo [64] reported a high influence of sodium tungstate, nickel sulphate and the interaction of sodium tungstate and nickel sulphate in controlling the corrosion behavior of Ni-W-P coatings. While for Ni-P-Cu coatings a dominant effect of nickel content was observed [65]. The present work is therefore in accordance with other research works [64,65]. Also, the low percentage contribution of error denotes that variability of experiments has been well captured in limited number of trials which justifies the use of  $L_9$  array.

**Table 8**

Confirmation tests for the initial and optimal parametric combination.

Ni-W-P			
	Initial	Optimal	
		Predicted	Experimental
Level	$A_1B_3C_3$	$A_3B_2C_2$	$A_3B_2C_2$
$E_{corr}$ (mV)	-391		-258
$I_{corr}$ ( $\mu A/cm^2$ )	0.5		0.065
GFG	0.645	0.9403	0.929
Improvement in grade = 0.284 (44.03 %)			
Ni-Cu-P			
	Initial	Optimal	
		Predicted	Experimental
Level	$A_2B_2C_2$	$A_1B_1C_1$	$A_1B_1C_1$
$E_{corr}$ (mV)	-356		-350
$I_{corr}$ ( $\mu A/cm^2$ )	0.78		0.4
GFG	0.81	0.9043	0.858
Improvement in grade = 0.048 (5.9 %)			

**Table 9**

Comparison of optimized results with bare rebar.

Sl. No.	Corrosion parameters	Bare rebar	Ni-W-P optimized	Ni-Cu-P optimized
1	$E_{corr}$ (mV)	-653	-258	-350
2	$I_{corr}$ ( $\mu A/cm^2$ )	11.7	0.065	0.4

**Table 10**

Analysis of variance of Ni-W-P and Ni-Cu-P coated rebars.

Ni-W-P					
Source	DF	Adj SS	Adj MS	F-Value	% Contribution
A	2	0.00	0.00	0.08	0.16
B	2	0.11	0.06	18.86	38.42
C	2	0.18	0.09	29.14	59.37
Error	2	0.01	0.00		2.04
Total	8	0.30			100.00
Ni-Cu-P					
Source	DF	Adj SS	Adj MS	F-Value	% Contribution
A	2	0.19	0.09	6.68	67.20
B	2	0.00	0.00	0.09	0.93
C	2	0.06	0.03	2.17	21.81
Error	2	0.03	0.01		10.07
Total	8	0.28			100.00

#### 4.4. Coating characterization

The Ni-W-P coated rebars were observed under SEM at the obtained optimality the image of which is shown in Fig. 5(a). The image of optimized Ni-Cu-P coated rebar is shown in Fig. 5(b). Both the coated rebars present a compact surface. The Ni-Cu-P coated rebars appear cloudy and are without any defects. In general, a compact coating present a higher corrosion resistance since corrosive media do not penetrate the substrate through grain boundaries. Both the coatings represent the globular or cauliflower like morphology observed for electroless nickel coatings [41–45,66]. Also the Ni-Cu-P compact mass of nodules were observed by Liu et al. [67]. The EDS analyses are summarized in Table 11. Both the coated rebars are in the high P region. A high W can be seen for Ni-W-P coated rebars. An increase in W is associated with a compact nodular structure [44,45]. Thus, the composition corroborates well with the coating morphology. Furthermore, the XRD of coated rebars at optimal condition is shown in Fig. 6. A mixed amorphous and nano-crystalline is concluded for both type of coated rebars. Literature suggests that for both coatings, crystallinity is improved with an increase in W or Cu concentration which may also favor the corrosion resistance and a sharp peak of Ni(111) is superimposed by a broad dome [44,45,66,67].

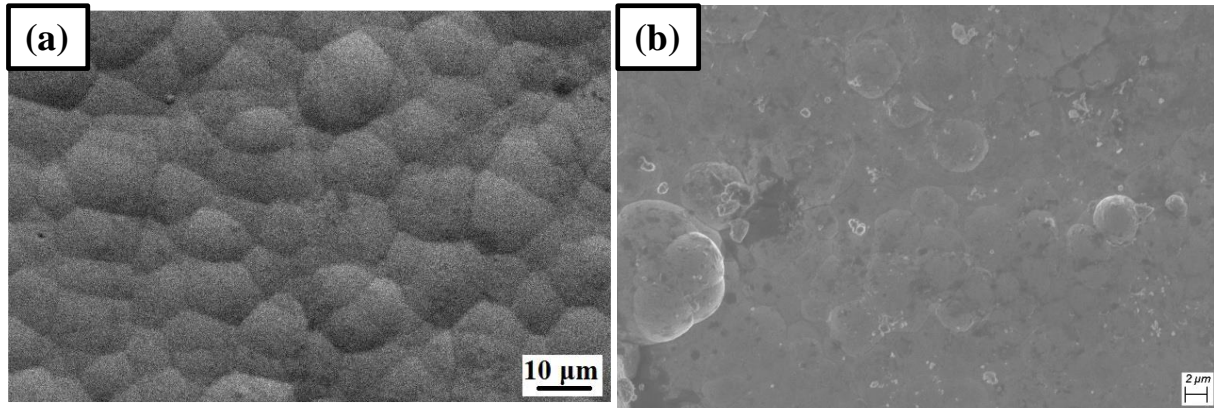


Fig. 5. SEM results of (a) Ni-W-P [44] and FESEM of (b) Ni-Cu-P [45] coated rebar at optimal condition.

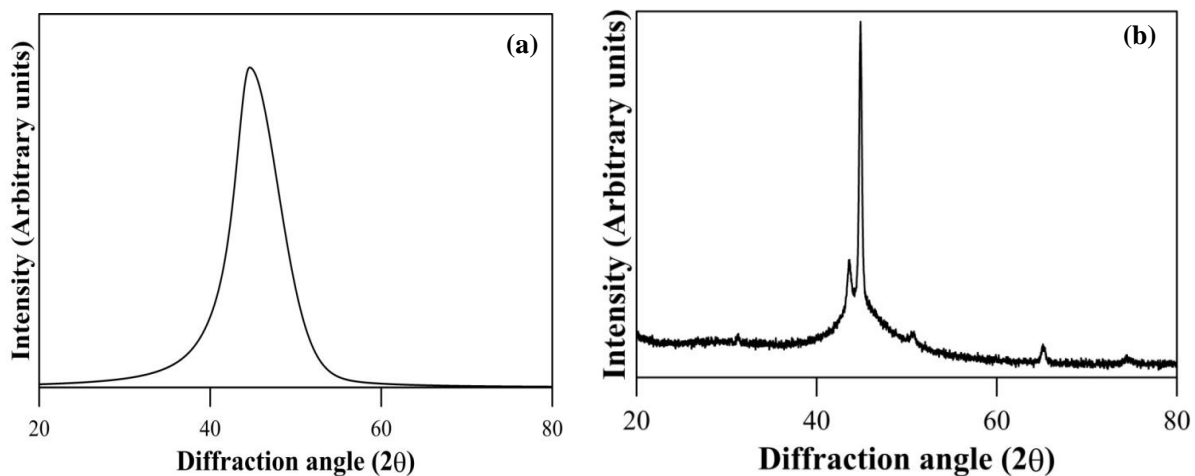


Fig. 6. XRD results of (a) Ni-W-P [44] and (b) Ni-Cu-P [45] coated rebar at optimal condition.

Table 11

EDS analysis of Ni-W-P and Ni-Cu-P coating at optimal condition.

Combination	Wt. % of Ni	Wt. % of P	Wt. % of W	Wt. % of Cu
Ni-W-P	83-85	8-9	7-8	×
Ni-Cu-P	85-88	9-11	×	3-4

#### 4.5. Corrosion mechanism

The corrosion mechanism is studied by observing the corroded specimens under SEM/FESEM and the results are shown in Fig. 7. The bare rebars were severely cracked due to chloride attack in Fig. 7(a). Deep pits are observed due to chloride attack. Thus, severity of the chloride attack leading to higher corrosion current (Table 9) is confirmed. Lamellar structures are seen on Ni-W-P coated rebars (optimal condition) subjected to electrochemical tests in Fig. 7(b) which is a consequence of passivation products. It seems there is initiation of passivation in the Ni-W-P coated rebars and expectedly the corrosion products are oxides of W or Ni [44]. Similar results are observed for Ni-Cu-P coated rebars in Fig. 7(c). Thus, initiation of passivation may be concluded which leads to an enhancement of corrosion resistance of rebars. Roy and Sahoo [65]

observed a cracked surface for Ni-Cu-P coatings optimized using GRA. But the use of grey fuzzy analysis in the present work resulted in effective bath optimization to achieve enhanced corrosion resistance of the rebars. The initiation of passivation in the optimized coated rebars may enhance the long-term protection ability in harsh chloride environment and may be investigated in future research works. The coating bath optimization also results in effective utilization of resources thereby improving cost-effectivity.

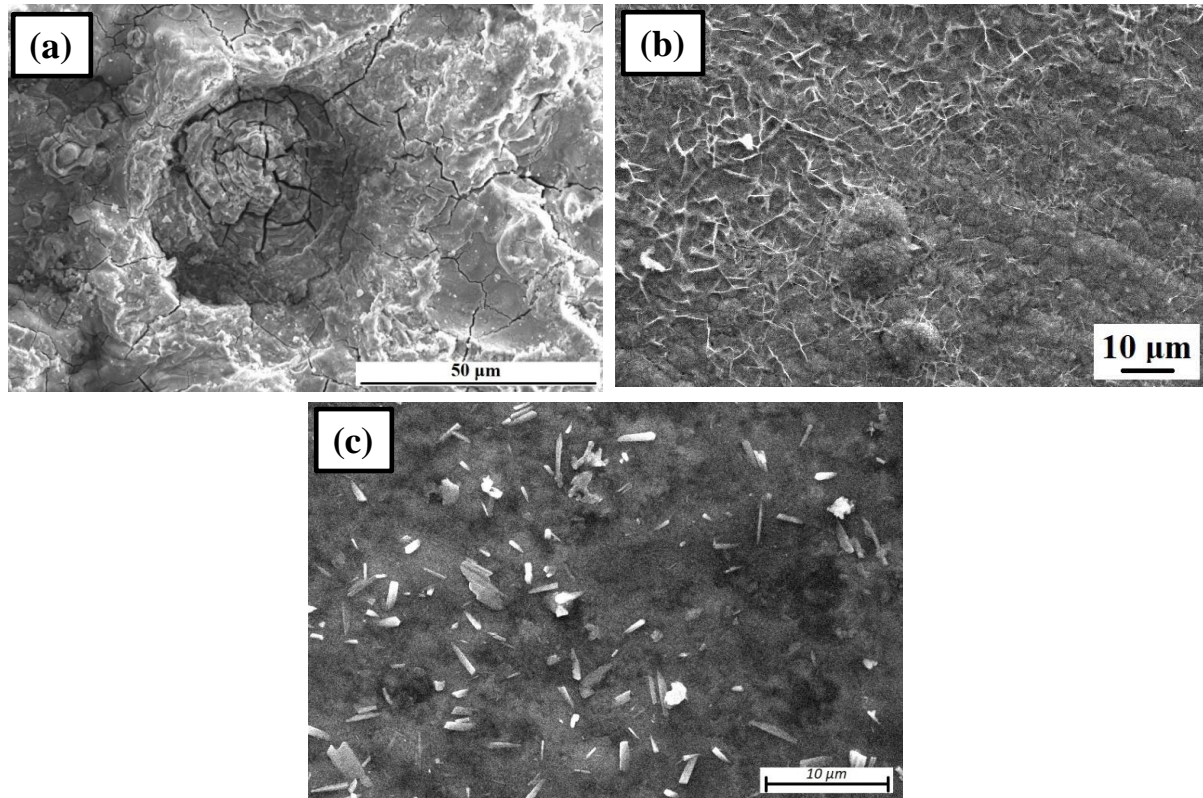


**Fig. 7.** SEM results of corroded (a) bare rebar and (b) Ni-W-P coated rebar at optimal combination. The FESEM result of corroded Ni-Cu-P at optimal condition is shown in (c) [42,44,45].

## 5. Conclusions

The applicability of optimized electroless coatings to improve lifetime of structures in marine environment was investigated. Taguchi's  $L_9$  orthogonal array was used to reduce the number of trials. The concentration of different constituents was varied to obtain coatings with different elemental weight percent. A hybrid grey fuzzy reasoning approach was proposed to optimize corrosion performance. For rebars with Ni-W-P coating,  $A_3B_2C_2$  and for rebars with Ni-Cu-P coating,  $A_1B_1C_1$  combination set results in optimal corrosion resistance. The  $E_{\text{corr}}$  and  $I_{\text{corr}}$  for optimized Ni-W-P coatings were seen to be  $-258$  mV and  $0.065 \mu\text{A}/\text{cm}^2$  respectively. While for Ni-Cu-P coatings the  $E_{\text{corr}}$  and  $I_{\text{corr}}$  was observed to be  $-350$  mV and  $0.4 \mu\text{A}/\text{cm}^2$  respectively. This was significantly lower compared to the bare rebars ( $E_{\text{corr}} = -653$  mV and  $I_{\text{corr}} = 11.7 \mu\text{A}/\text{cm}^2$ ). ANOVA results indicate that W concentration has highest influence (59.37%) for Ni-W-P coated rebar while for Ni-Cu-P coating the Ni concentration has highest significance (67.20%) in controlling corrosion. The optimized coatings have a compact and defect free structure which

enhances corrosion resistance. The corroded surfaces indicate severe cracking due to chloride induced attack on bare Fe-600 grade rebars. While passivation products are observed on the coated rebars which improve the corrosion resistance. Thus, the ternary and optimized coating variants used in the present work may prove to be worthy low cost alternatives to laser clad materials or stainless steel or nickel / monel alloys used in construction industry for mitigation of corrosion.

Further research work may be carried out to investigate corrosion performance in long-term and effect of carbonation on the coating performance. The present work optimizes electroless Ni-W-P and Ni-Cu-P coatings to achieve enhanced corrosion resistance of the Fe-600 grade rebars in 3.5% NaCl. But there are other environments where construction grade rebars find usage such as in food processing industries where there is attack of sulphate species. So, the coatings must be optimized to cater into varying corrosive environments. Also, the corrosive media should be aerated to account for harmful effects of carbon dioxide acting synergistically with chloride or sulphate species. Such challenges would be taken up in future research works to make the coatings suitable for industrial adoption. The present work is a preliminary investigation to optimize the coatings and initial steps towards bath standardization which has shown the tremendous potential of electroless Ni-P based coatings as potential candidates. So further research works will be carried out to enhance the coating properties in long run and for long term corrosion protection.

## **Acknowledgments**

The authors gratefully acknowledge the coating characterization facility provided by Central Instrumentation Facility (CIF) of Birla Institute of Technology, Mesra, Ranchi – 835215.

## **Funding**

This research received no external funding.

## **Conflicts of interest**

The authors declare no conflict of interest.

## **Authors contribution statement**

AM, SS: Conceptualization; AM: Data curation; AM: Formal analysis; AM, SS: Investigation; AM, SS: Methodology; SS: Project administration; SS: Resources; AM: Software; SS: Supervision; AM, SS: Validation; SS: Visualization; AM: Roles/Writing – original draft; SS: Writing – review & editing.

## **References**

- [1] Sanjurjo A, Hettiarachchi S, Lau KH, Cox P, Wood B. Coatings for corrosion protection of steel used in reinforced concrete. *Surf Coatings Technol* 1992;54–55:224–8.

- [https://doi.org/10.1016/S0257-8972\(09\)90054-8](https://doi.org/10.1016/S0257-8972(09)90054-8).
- [2] Pei X, Noël M, Fam A, Green M. Development length of steel reinforcement with corrosion protection cementitious coatings. *Cem Concr Compos* 2015;60:34–43. <https://doi.org/10.1016/j.cemconcomp.2015.04.003>.
- [3] Song Y, Wightman E, Kulandaivelu J, Bu H, Wang Z, Yuan Z, et al. Rebar corrosion and its interaction with concrete degradation in reinforced concrete sewers. *Water Res* 2020;182:115961. <https://doi.org/10.1016/j.watres.2020.115961>.
- [4] Samson G, Deby F, Garcia J-L, Lassoued M. An alternative method to measure corrosion rate of reinforced concrete structures. *Cem Concr Compos* 2020;112:103672. <https://doi.org/10.1016/j.cemconcomp.2020.103672>.
- [5] Cabrini M, Lorenzi S, Coffetti D, Coppola L, Pastore T. Inhibition Effect of Tartrate Ions on the Localized Corrosion of Steel in Pore Solution at Different Chloride Concentrations. *Buildings* 2020;10:105. <https://doi.org/10.3390/buildings10060105>.
- [6] Bolzoni F, Brenna A, Beretta S, Ormellesse M, Diamanti M V, Pedefferri MP. Progresses in prevention of corrosion in concrete. *IOP Conf. Ser. Earth Environ. Sci.*, vol. 296, IOP Publishing; 2019, p. 12016.
- [7] Sadati S, Arezoumandi M, Shekarchi M. Long-term performance of concrete surface coatings in soil exposure of marine environments. *Constr Build Mater* 2015;94:656–63. <https://doi.org/10.1016/j.conbuildmat.2015.07.094>.
- [8] James A, Bazarchi E, Chiniforush AA, Panjebashi Aghdam P, Hosseini MR, Akbarnezhad A, et al. Rebar corrosion detection, protection, and rehabilitation of reinforced concrete structures in coastal environments: A review. *Constr Build Mater* 2019;224:1026–39. <https://doi.org/10.1016/j.conbuildmat.2019.07.250>.
- [9] Sagüés AA, Pech-Canul MA, Shahid Al-Mansur AKM. Corrosion macrocell behavior of reinforcing steel in partially submerged concrete columns. *Corros Sci* 2003;45:7–32. [https://doi.org/10.1016/S0010-938X\(02\)00087-2](https://doi.org/10.1016/S0010-938X(02)00087-2).
- [10] Shi J, Ming J. Influence of defects at the steel-mortar interface on the corrosion behavior of steel. *Constr Build Mater* 2017;136:118–25. <https://doi.org/10.1016/j.conbuildmat.2017.01.007>.
- [11] Pradhan B, Bhattacharjee B. Rebar corrosion in chloride environment. *Constr Build Mater* 2011;25:2565–75. <https://doi.org/10.1016/j.conbuildmat.2010.11.099>.
- [12] Manera M, Vennesland Ø, Bertolini L. Chloride threshold for rebar corrosion in concrete with addition of silica fume. *Corros Sci* 2008;50:554–60. <https://doi.org/10.1016/j.corsci.2007.07.007>.
- [13] Wang D, Ming J, Shi J. Enhanced corrosion resistance of rebar in carbonated concrete pore solutions by Na<sub>2</sub>HPO<sub>4</sub> and benzotriazole. *Corros Sci* 2020;174:108830. <https://doi.org/10.1016/j.corsci.2020.108830>.
- [14] Wu M, Shi J. Beneficial and detrimental impacts of molybdate on corrosion resistance of steels in alkaline concrete pore solution with high chloride contamination. *Corros Sci* 2021;183:109326. <https://doi.org/10.1016/j.corsci.2021.109326>.
- [15] Kumar S, Yang E-H, Unluer C. Investigation of chloride penetration in carbonated reactive magnesia cement mixes exposed to cyclic wetting–drying. *Constr Build Mater* 2021;284:122837. <https://doi.org/10.1016/j.conbuildmat.2021.122837>.
- [16] Cascudo O, Pires P, Carasek H, de Castro A, Lopes A. Evaluation of the pore solution of concretes with mineral additions subjected to 14 years of natural carbonation. *Cem Concr Compos* 2021;115:103858. <https://doi.org/10.1016/j.cemconcomp.2020.103858>.
- [17] Liu S, Zhu M, Ding X, Ren Z, Zhao S, Zhao M, et al. High-Durability Concrete with Supplementary Cementitious Admixtures Used in Corrosive Environments. *Crystals* 2021;11:196. <https://doi.org/10.3390/cryst11020196>.
- [18] Baltazar-Zamora MA, Bastidas D, Santiago-Hurtado G, Mendoza-Rangel JM, Gaona-Tiburcio

- C, Bastidas JM, et al. Effect of Silica Fume and Fly Ash Admixtures on the Corrosion Behavior of AISI 304 Embedded in Concrete Exposed in 3.5% NaCl Solution. *Materials (Basel)* 2019;12:4007. <https://doi.org/10.3390/ma12234007>.
- [19] Söylev TA, Richardson MG. Corrosion inhibitors for steel in concrete: State-of-the-art report. *Constr Build Mater* 2008;22:609–22. <https://doi.org/10.1016/j.conbuildmat.2006.10.013>.
- [20] Pan C, Chen N, He J, Liu S, Chen K, Wang P, et al. Effects of corrosion inhibitor and functional components on the electrochemical and mechanical properties of concrete subject to chloride environment. *Constr Build Mater* 2020;260:119724. <https://doi.org/10.1016/j.conbuildmat.2020.119724>.
- [21] Luo H, Su H, Dong C, Li X. Passivation and electrochemical behavior of 316L stainless steel in chlorinated simulated concrete pore solution. *Appl Surf Sci* 2017;400:38–48. <https://doi.org/10.1016/j.apsusc.2016.12.180>.
- [22] Tian Y, Liu M, Cheng X, Dong C, Wang G, Li X. Cr-modified low alloy steel reinforcement embedded in mortar for two years: Corrosion result of marine field test. *Cem Concr Compos* 2019;97:190–201. <https://doi.org/10.1016/j.cemconcomp.2018.12.019>.
- [23] Mukhopadhyay A, Sahoo S. Corrosion Protection of Construction Steel. *Handb. Res. Dev. Trends Ind. Mater. Eng.*, IGI Global; 2020, p. 327–47.
- [24] Tang F, Chen G, Brow RK, Volz JS, Koenigstein ML. Corrosion resistance and mechanism of steel rebar coated with three types of enamel. *Corros Sci* 2012;59:157–68. <https://doi.org/10.1016/j.corsci.2012.02.024>.
- [25] Tang F, Chen G, Volz JS, Brow RK, Koenigstein M. Microstructure and corrosion resistance of enamel coatings applied to smooth reinforcing steel. *Constr Build Mater* 2012;35:376–84. <https://doi.org/10.1016/j.conbuildmat.2012.04.059>.
- [26] Gao Z. Corrosion damage of reinforcement embedded in reinforced concrete slab 2016.
- [27] Tang F, Chen G, Brow RK. Chloride-induced corrosion mechanism and rate of enamel- and epoxy-coated deformed steel bars embedded in mortar. *Cem Concr Res* 2016;82:58–73. <https://doi.org/10.1016/j.cemconres.2015.12.015>.
- [28] Pour-Ali S, Dehghanian C, Kosari A. Corrosion protection of the reinforcing steels in chloride-laden concrete environment through epoxy/polyaniline–camphorsulfonate nanocomposite coating. *Corros Sci* 2015;90:239–47. <https://doi.org/10.1016/j.corsci.2014.10.015>.
- [29] Sohail MG, Salih M, Al Nuaimi N, Kahraman R. Corrosion performance of mild steel and epoxy coated rebar in concrete under simulated harsh environment. *Int J Build Pathol Adapt* 2019;37:657–78. <https://doi.org/10.1108/IJBPA-12-2018-0099>.
- [30] Rajitha K, Mohana KNS, Mohanan A, Madhusudhana AM. Evaluation of anti-corrosion performance of modified gelatin-graphene oxide nanocomposite dispersed in epoxy coating on mild steel in saline media. *Colloids Surfaces A Physicochem Eng Asp* 2020;587:124341. <https://doi.org/10.1016/j.colsurfa.2019.124341>.
- [31] Khodair ZT, Khadom AA, Jasim HA. Corrosion protection of mild steel in different aqueous media via epoxy/nanomaterial coating: preparation, characterization and mathematical views. *J Mater Res Technol* 2019;8:424–35. <https://doi.org/10.1016/j.jmrt.2018.03.003>.
- [32] Tang F, Bao Y, Chen Y, Tang Y, Chen G. Impact and corrosion resistances of duplex epoxy/enamel coated plates. *Constr Build Mater* 2016;112:7–18. <https://doi.org/10.1016/j.conbuildmat.2016.02.170>.
- [33] Wang Y, Kong G, Che C, Zhang B. Inhibitive effect of sodium molybdate on the corrosion behavior of galvanized steel in simulated concrete pore solution. *Constr Build Mater* 2018;162:383–92. <https://doi.org/10.1016/j.conbuildmat.2017.12.035>.
- [34] Pokorný P, Tej P, Kouřil M. Evaluation of the impact of corrosion of hot-dip galvanized reinforcement on bond strength with concrete – A review. *Constr Build Mater* 2017;132:271–89. <https://doi.org/10.1016/j.conbuildmat.2016.11.096>.

- [35] Li L, Wang J, Xiao J, Yan J, Fan H, Sun L, et al. Time-dependent corrosion behavior of electroless Ni-P coating in H<sub>2</sub>S/Cl<sup>-</sup> environment. *Int J Hydrogen Energy* 2021;46:11849–64. <https://doi.org/10.1016/j.ijhydene.2021.01.053>.
- [36] Li J, Zeng H, Luo J-L. Probing the corrosion resistance of a smart electroless Ni-P composite coating embedded with pH-responsive corrosion inhibitor-loaded nanocapsules. *Chem Eng J* 2021;421:127752. <https://doi.org/10.1016/j.cej.2020.127752>.
- [37] Yu Q, Zhou T, He Y, Liu P, Wang X, Jiang Y, et al. Annealed high-phosphorus electroless Ni-P coatings for producing molds for precision glass molding. *Mater Chem Phys* 2021;262:124297. <https://doi.org/10.1016/j.matchemphys.2021.124297>.
- [38] Cui C, Du H, Liu H, Xiong T. Corrosion behavior of the electroless Ni-P coating on the pore walls of the lotus-type porous copper. *Corros Sci* 2020;162:108202. <https://doi.org/10.1016/j.corsci.2019.108202>.
- [39] Verdi P, Monirvaghefi SM. Electroless Ni-P Plating of Carbon Steel via Hot Substrate Method and Comparison of Coating Properties with those for Conventional Method. *J Mater Eng Perform* 2020;29:7915–28. <https://doi.org/10.1007/s11665-020-05286-8>.
- [40] Krishnan KH, John S, Srinivasan KN, Praveen J, Ganesan M, Kavimani PM. An overall aspect of electroless Ni-P depositions—A review article. *Metall Mater Trans A* 2006;37:1917–26. <https://doi.org/10.1007/s11661-006-0134-7>.
- [41] Singh DDN, Ghosh R. Electroless nickel-phosphorus coatings to protect steel reinforcement bars from chloride induced corrosion. *Surf Coatings Technol* 2006;201:90–101. <https://doi.org/10.1016/j.surfcoat.2005.10.045>.
- [42] Mukhopadhyay A, Sahoo S. Corrosion protection of reinforcement steel rebars by the application of electroless nickel coatings. *Eng Res Express* 2019;1:15021.
- [43] Mukhopadhyay A, Sahoo S. Improving corrosion resistance of reinforcement steel rebars exposed to sulphate attack by the use of electroless nickel coatings. *Eur J Environ Civ Eng* 2021;1–16. <https://doi.org/10.1080/19648189.2021.1886177>.
- [44] Mukhopadhyay A, Sahoo S. Corrosion performance of steel rebars by application of electroless Ni-PW coating: An optimization approach using grey relational analysis. *FME Trans* 2021;49:445–55.
- [45] Mukhopadhyay A, Sahoo S. Optimized electroless Ni-Cu-P coatings for corrosion protection of steel rebars from pitting attack of chlorides. *Eng Trans* 2021;69:315–32.
- [46] Sajid HU, Kiran R, Bajwa DS. Soy-protein and corn-derived polyol based coatings for corrosion mitigation in reinforced concrete. *Constr Build Mater* 2022;319:126056. <https://doi.org/10.1016/j.conbuildmat.2021.126056>.
- [47] Sharma N, Sharma S, Sharma SK, Mahajan RL, Mehta R. Evaluation of corrosion inhibition capability of graphene modified epoxy coatings on reinforcing bars in concrete. *Constr Build Mater* 2022;322:126495. <https://doi.org/10.1016/j.conbuildmat.2022.126495>.
- [48] Lin J., Lin C. The use of the orthogonal array with grey relational analysis to optimize the electrical discharge machining process with multiple performance characteristics. *Int J Mach Tools Manuf* 2002;42:237–44. [https://doi.org/10.1016/S0890-6955\(01\)00107-9](https://doi.org/10.1016/S0890-6955(01)00107-9).
- [49] T M, P R, Es G, P S, Ksr. A. Experimental Investigation of Coconut Oil with Nanoboric Acid During Milling of Inconel 625 Using Taguchi-Grey Relational Analysis. *Surf Rev Lett* 2021;28:2150008. <https://doi.org/10.1142/S0218625X21500086>.
- [50] Nagaraj Y, Jagannatha N, Sathisha N, Niranjana SJ. Parametric optimization on hot air assisted hybrid machining of soda-lime glass using Taguchi based grey relational analysis. *Multiscale Multidiscip Model Exp Des* 2021;4:169–85. <https://doi.org/10.1007/s41939-020-00085-z>.
- [51] Lian G, Xiao S, Zhang Y, Jiang J, Zhan Y. Multi-objective optimization of coating properties and cladding efficiency in 316L/WC composite laser cladding based on grey relational analysis. *Int J Adv Manuf Technol* 2021;112:1449–59. <https://doi.org/10.1007/s00170-020-06486-1>.

- [52] Prasath V, Krishnaraj V, Geetha Priyadarshini B, Kanchana J. Multi-objective optimization of Pulsed direct current magnetron sputtered titanium nitride thin film using Grey relational analysis. *Proc Inst Mech Eng Part L J Mater Des Appl* 2021;235:100–13. <https://doi.org/10.1177/1464420720951899>.
- [53] LA. Z. Fuzzy sets. *Information Control* 1965;8:338–353.
- [54] Kumar H, Harsha A. Taguchi optimization of various parameters for tribological performance of polyalphaolefins based nanolubricants. *Proc Inst Mech Eng Part J J Eng Tribol* 2021;235:1262–80. <https://doi.org/10.1177/1350650120972294>.
- [55] Nguyen H-P, Pham V-D. Single objective optimization of die- sinking electrical discharge machining with low frequency vibration assigned on workpiece by taguchi method. *J King Saud Univ - Eng Sci* 2021;33:37–42. <https://doi.org/10.1016/j.jksues.2019.11.001>.
- [56] Sharifi E, Sadjadi SJ, Aliha MR., Moniri A. Optimization of high-strength self-consolidating concrete mix design using an improved Taguchi optimization method. *Constr Build Mater* 2020;236:117547. <https://doi.org/10.1016/j.conbuildmat.2019.117547>.
- [57] Dagdevir T, Ozceyhan V. Optimization of process parameters in terms of stabilization and thermal conductivity on water based TiO<sub>2</sub> nanofluid preparation by using Taguchi method and Grey relation analysis. *Int Commun Heat Mass Transf* 2021;120:105047. <https://doi.org/10.1016/j.icheatmasstransfer.2020.105047>.
- [58] Kumaran ST, Ko TJ, Kurniawan R. Grey fuzzy optimization of ultrasonic-assisted EDM process parameters for deburring CFRP composites. *Measurement* 2018;123:203–12. <https://doi.org/10.1016/j.measurement.2018.03.076>.
- [59] Soepangkat BOP, Pramujati B, Effendi MK, Norcahyo R, Mufarrih AM. Multi-objective Optimization in Drilling Kevlar Fiber Reinforced Polymer Using Grey Fuzzy Analysis and Backpropagation Neural Network–Genetic Algorithm (BPNN–GA) Approaches. *Int J Precis Eng Manuf* 2019;20:593–607. <https://doi.org/10.1007/s12541-019-00017-z>.
- [60] Siva Sankara Raju, Srinivasa Rao G, Samantra C. Wear behavioral assessment of Al-CSAp-MMCs using grey-fuzzy approach. *Measurement* 2019;140:254–68. <https://doi.org/10.1016/j.measurement.2019.04.004>.
- [61] Moganapriya C, Rajasekar R, Sathish Kumar P, Mohanraj T, Gobinath VK, Saravanakumar J. Achieving machining effectiveness for AISI 1015 structural steel through coated inserts and grey-fuzzy coupled Taguchi optimization approach. *Struct Multidiscip Optim* 2021;63:1169–86. <https://doi.org/10.1007/s00158-020-02751-9>.
- [62] Gao Z, Li J. Fuzzy Analytic Hierarchy Process Evaluation Method in Assessing Corrosion Damage of Reinforced Concrete Bridges. *Civ Eng J* 2018;4:843. <https://doi.org/10.28991/cej-0309138>.
- [63] Mukhopadhyay A, Duari S, Barman TK, Sahoo P. Optimization of Friction and Wear Properties of Electroless Ni–P Coatings Under Lubrication Using Grey Fuzzy Logic. *J Inst Eng Ser D* 2017;98:255–68. <https://doi.org/10.1007/s40033-016-0133-9>.
- [64] Roy S, Sahoo P. Potentiodynamic Polarization Behaviour of Electroless Ni-P-W Coatings. *ISRN Corros* 2012;2012:1–11. <https://doi.org/10.5402/2012/914867>.
- [65] Roy S, Sahoo P. Parametric optimization of corrosion and wear of electroless Ni-P-Cu coating using grey relational coefficient coupled with weighted principal component analysis. *Int J Mech Mater Eng* 2014;9:10. <https://doi.org/10.1186/s40712-014-0010-y>.
- [66] Balaraju JN, Kalavati, Rajam KS. Surface morphology and structure of electroless ternary NiWP deposits with various W and P contents. *J Alloys Compd* 2009;486:468–73. <https://doi.org/10.1016/j.jallcom.2009.06.173>.
- [67] Liu J, Wang X, Tian Z, Yuan M, Ma X. Effect of copper content on the properties of electroless Ni–Cu–P coatings prepared on magnesium alloys. *Appl Surf Sci* 2015;356:289–93. <https://doi.org/10.1016/j.apsusc.2015.08.072>.